Ceramics International 42 (2016) 13642–13647

Contents lists available at ScienceDirect

Ceramics International

journal homepage: www.elsevier.com/locate/ceramint

# Microstructural and multiferroic properties in layered perovskite-related $Sm_6Ti_4Fe_2O_{20}$

Xiangyi Cheng [a], Chao Ma [b,*], Xiaoxiong Wang [a], Dechao Meng [b], Jiangluqi Song [a], Hongshun Yang [a], Keqing Ruan [a,*]

[a] *Key Laboratory of Strongly-Coupled Quantum Matter Physics, Chinese Academy of Sciences, and School of Physical Sciences, University of Science and Technology of China, Hefei 230026, China*

[b] *Hefei National Laboratory for Physical Sciences at Microscale, University of Science and Technology of China, Hefei 230026, China*

## ARTICLE INFO

*Article history:*
Received 14 April 2016
Received in revised form
24 May 2016
Accepted 24 May 2016
Available online 25 May 2016

*Keywords:*
Layered perovskite-related oxide
Multiferroics
Scanning transmission electron microscopy
Spin glass-like behavior

## ABSTRACT

Layered perovskite-related $Sm_6Ti_4Fe_2O_{20}$ compound was successfully synthesized through the intercalation of bilayer $SmFeO_3$ into the $Sm_2Ti_2O_7$ with pyrochlore structure by means of floating-zone melting technique. The microstructural properties were characterized using aberration-corrected scanning transmission electron microscopy and X-ray diffraction. Electron energy-loss spectroscopy investigation reveals that the $Fe^{3+}$ ions prefer to occupy the inner sites within the perovskite-like layers. This compound exhibits clearly the spin glass-like behavior as demonstrated by the magnetic properties measurement. Such complex magnetic behavior could be attributed to the partial chemical order of Ti/Fe over the B sites and the interactions between magnetic ions including $Sm^{3+}$ and $Fe^{3+}$. In addition, the multiferroic behavior with the coexistence of the ferroelectricity and ferromagnetism was well established by magnetic and piezoresponse measurements.

## 1. Introduction

The lanthanide dititanate family, $Ln_2Ti_2O_7$, has two possible types of structure, if Ln are rare earth elements with large ionic radius including La, Ce, Pr, and Nd, the compound formed will adopt a (110)-layered perovskite structure and be well known for their ferroelectric and piezoelectric properties widely used for the elaboration of high temperature devices [1–4]. If the ratio of the cation radii between $Ln^{3+}$ and $Ti^{4+}$ is in the range of 1.46–1.78, then the compound formed will prefer a pyrochlore structure with the $Fd\bar{3}m$ space group. For instance, $Ln_2Ti_2O_7$ (with Ln=Sm to Lu) crystallize in this structure and attract considerable interest due to the exotic magnetic phases such as spin ice and spin liquid [5–9]. Multiferroic materials, exhibiting ferroelectric and magnetic orders simultaneously, have been a subject of intense study in the recent years, duo to their significance for fundamental physics and technological application such as memory and sensors [10–13]. In the search of the single-phase multiferroic compounds, one effective approach which has been verified is to intercalate magnetic species into the central octahedron layer of ferroelectric hosts, while maintaining ferroelectric displacements in the outer octahedron layers [14–18]. In layered perovskite-related series $A_nB_nO_{3n+2}$, $La_2Ti_2O_7$ constitutes an example of layered perovskite, which has four layer per block, and it is also a ferroelectric material with high Curie temperature [19–21]. Based on the incorporation of perovskite-like $LaFeO_3$ into a $La_2Ti_2O_7$ matrix, single crystal of $La_6Ti_4Fe_2O_{20}$ with layered structure of the n=6 type has successfully prepared and investigated preliminarily by F. Lichtenberg and A. Wölfe et al. [22–24]. Further, the multiferroic properties have been well confirmed by recent study [25].

In the bulk, the stable structure of $Sm_2Ti_2O_7$ is pyrochlore and belongs to the $Fd\bar{3}m$ space group [26]. The (110)-layered perovskite structure of this compound has, however, been synthesized by using high pressure techniques, pulsed laser deposition and the sol–gel route [27–30]. The metastable $Sm_2Ti_2O_7$ phase crystallizes in the monoclinic structure (layered perovskite structure) with $P2_1$ space group and is isostructural to $La_2Ti_2O_7$. Recently, for the first time, the ferroelectric character of metastable phase has been revealed at the nanoscale level by piezoresponse force microscopy [27].

The recent fundamental technological breakthroughs in electron microscopy with the correction of electron-optical aberrations provides a feasible access to a direct interpretation of the atomic structure at subangstrom resolution, and this technique gives us a new insight into the structure determination of layered structures at atomic scale [31,32]. Moreover, the combination of scanning transmission electron microscopy (STEM) images and electron energy-loss spectroscopy (EELS) enables the analysis of

---

* Corresponding authors.
*E-mail addresses:* cma@ustc.edu.cn (C. Ma), kqruan@ustc.edu.cn (K. Ruan).

http://dx.doi.org/10.1016/j.ceramint.2016.05.159

chemically sensitive information at atomic resolution, such as the inhomogeneous distribution of magnetic-cation in the layered structures. In the present work, we have grown the layered perovskite-related oxide $Sm_6Ti_4Fe_2O_{20}$ successfully via the insertion of two layers of $SmFeO_3$ into $Sm_2Ti_2O_7$. By combining STEM images and EELS measurements, the microstructure character as well as the magnetic cation distribution was directly imaged. The magnetic properties of six-layered $Sm_6Ti_4Fe_2O_{20}$ have been investigated. Besides, the weak ferromagnetic and ferroelectric properties have been confirmed at room temperature.

## 2. Experimental details

The $Sm_6Ti_4Fe_2O_{20}$ single crystals were prepared by floating-zone melting technique [22]. The stoichiometric amounts of predried powders of $Sm_2O_3$, $TiO_2$ and $Fe_2O_3$ were mixed thoroughly, and the mixtures were calcined at 1400 °C for 12 h. The resulting powders were milled and isostatically pressed into two cylindrical rods under 50 MPa. The product was fired a further 12 h at the same temperature. Single-crystallines rods were grown in a four-mirror optical- floating-zone furnace (FZ-T-4000-H, Crystal Systems Corp.) using four 1 kW halogen lamps as the infrared radiation source with flowing air. During the growth process, the molten zone moved upwards at a rate of 15 mm $h^{-1}$, with the seed rod (lower shaft) and the feed rod (upper shaft) counter rotating at 25 rpm in air flow of 5 L $h^{-1}$ [25].

The crystal structure of the obtained sample was firstly characterized by X-ray diffraction (XRD) experiments (Rigaku D/Max-rA) employing Cu Kα radiation ($\lambda = 1.5418$ Å). The STEM and EELS measurements were carried out on a JEOL ARM200F transmission electron microscope (TEM) equipped with a probe-forming aberration corrector and Gatan image filter (Quantum 965). The temperature dependence of magnetization was carried out using a superconducting quantum interference device (SQUID, MPMS, Quantum Design) magnetometer measured from 5 to 400 K. The magnetization hysteresis measurements were performed on a SQUID-VSM (SVSM, Quantum Design) over an applied magnetic field range of $\pm 70$ kOe at 5 K and 300 K. For the piezoresponse measurements, the obtained crystal rod was ground, pelletized, and fired at 1400 °C for 24 h. The pellets of $Sm_6Ti_4Fe_2O_{20}$ were polished by the metallographic sandpaper. The surface morphology and roughness of the polished sample were determined by Atomic Force Microscopy (AFM) in the contact mode, using a commercial microscope (Bruker). Local piezoresponse loops and ferroelectric domain structure were carried out using the spectroscopic tool of AFM with a conductive tip coating and a ground conductive substrate at room temperature.

## 3. Results and discussion

The $A_nB_nO_{3n+2}$ phases usually has layered structures consisting of (110) slabs of perovskite structure separated by additional layers of O atoms, with adjacent slabs offset by half the body diagonal of an octahedron along **a** with respect to each other. The width of the slabs in terms of the number of octahedra can be obtained by the parameter n in the chemical formula directly [22]. The XRD pattern obtained at room temperature for $Sm_6Ti_4Fe_2O_{20}$ is shown in Fig. 1. The position of the peaks in the range of low diffraction angles indicates the characteristic of a layered structure belonging to the n=6 member [20]. The peaks can be indexed on the basis of a primitive orthorhombic cell, the calculated crystal parameters are a=7.76 Å, b=5.60 Å, and c=36.68 Å close to that of $La_6Ti_4Fe_2O_{20}$ [25].

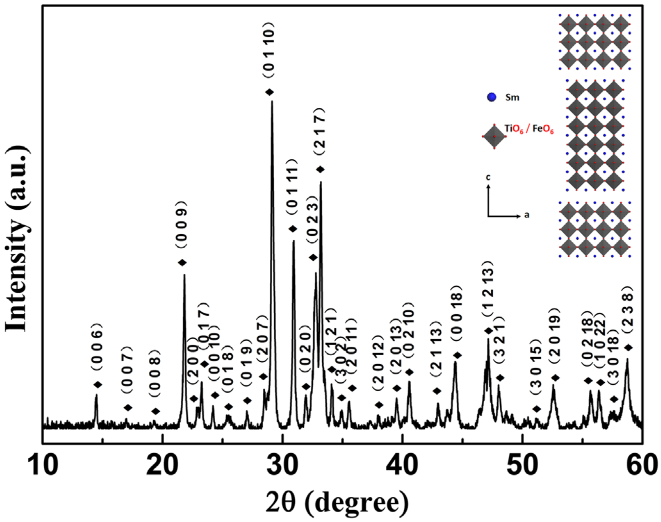

**Fig. 1.** XRD pattern of $Sm_6Ti_4Fe_2O_{20}$ and schematic of crystal structure.

In order to directly determine the layered character of this compound, we recorded the selected area electron diffraction (SAED) patterns and atomic-resolution high-angle annular dark field (HAADF) STEM images along different zone axes, as shown in Fig. 2. Three different zone-axis SAED patterns, i.e., the [0,1,1], [0 1 0], and [0–2] zone axes which are all parallel to the $ABO_3$ layers, can be well indexed using the cell parameters obtained from the XRD analysis. The primary reflections seen in Fig. 2a-c correspond to the form factor of the (Ti, Fe)$O_6$ octahedron, octahedron (with edge d*). Due to the space caused by shifted slabs in the $A_nB_nO_{3n+2}$ phase, the reciprocal distance d* between the direct beam (0 0 0) and the primary reflection in the c direction would be subdivided into (n+1) equal parts [33]. It can be seen clearly from Fig. 2b, the fundamental distance d* along [001] is subdivided into seven parts, indicating a slab thickness of six octahedral (n=6). It should be noted that the n=5 intergrowth was also observed in the some regions, as indicated by the streaking in the SAED pattern taken along the [0–2] zone axis (Fig. 2c). The structure can be inferred directly from the HAADF imagines, taken along the same direction as the SAED patterns, as illustrated in Fig. 2d-f. In this imaging condition, the brightness of atomic columns is approximately proportional to $Z^{1.7}$ (where Z is the atomic number) [34], and the oxygen atoms are invisible. Therefore, the brightest spots in these HAADF-STEM images correspond to the heaviest Sm atoms (green spheres), and the slightly bright spots arise from the Ti/Fe columns (yellow spheres), as shown by the structure model superimposed in the experimental image (Fig. 2e). It was clearly found that there are six oxygen octahedron layers per block along the [0 0 1] direction, suggesting that the n=6 member is derived from regular perovskite blocks with six octahedral layers per block. At the crystallographic shear planes, the pattern is broken and two rows of atoms give a square pattern.

Another important feature in this compound is the distribution of transition metal cations (Ti and Fe), which plays a critical role in the magnetic properties. From the enlarged HAADF image (Fig. 3a), it can be seen that the brightness in the Ti/Fe columns is not uniform, with higher intensity in the central part of each perovskite block. The intensity profile, scanning along the [0 0 1] direction indicated by a red rectangle, show more clearly the nonuniform intensity, as shown in Fig. 3b. Since the thickness in such small area is identical and the atomic number of Fe is larger than that of Ti, this intensity distribution directly reflects the distribution of the Ti and Fe, i.e., more Fe ions are located in the center of the perovskite block and the majority of Ti ions in the edge of the perovskite block. In order to further confirm this